OPEN ACCESS

Experimental Investigation of Hydraulic Jump Parameters in Sill Application Mode with Various Synthesis

Hamidreza Abbaszadeh [1]
Rasoul Daneshfaraz [2]
Reza Norouzi [1]

Abstract

Here, the effect of sill application on hydraulic jump parameters has been investigated. The model of sills is made of polyethylene in various dimensions. The sills were investigated in different positions relative to the gate in single, double, and triple arrangements. In a certain opening, the sill leads to more energy dissipation. By increasing the ratio of initial depth to sequent depth, the $\Delta E_{AB}/y_A$ decreases. It occurs due to the convergence of initial and sequent depths. In the under gate suppressed sill state, the $\Delta E_{AB}/E_A$ is 11.05% more than the upstream tangential position, while it's 14.56% for downstream specific energy. The results showed that the energy dissipation decreases with increasing the opening by at most 34.88%. In the same opening of no-sill and with sill cases, the use of suppressed sill leads to a decrease in the sequent depth compared to the no-sill one. The application of the sill causes an increase in the initial depth and accordingly the initial specific energy decreases; therefore, the sill leads to the reduction of the specific energy in the flow conjugate depths. The regression nonlinear polynomial equations were proposed to estimate the relative energy dissipation. Statistical indicators Relative Error (RE), Root Mean Square Error (RMSE), and Kling Gupta Efficiency (KGE) have been used to check the accuracy of presented equations. The mean RE% and RMSE for presented equation of $\Delta E_{AB}/E_A$ are 0.78%, and 0.004, respectively. These values are 0.87%, and 0.009 for $\Delta E_{AB}/E_B$, respectively. The KGE is in very good range for equations.

Keywords: Relative energy dissipation, Sequent depth, Hydraulic jump, Nonlinear regression equations.

1. Introduction

Sluice gates are one of the hydraulic structures that are widely used in irrigation networks due to their ease of use. These structures are used to measure the flow and regulate the upstream water level in open channels. Determining the hydraulic characteristics of the flow is one of the most

[1] Department of Civil Engineering, Faculty of Engineering, University of Maragheh, Maragheh, Iran.
[2] Department of Civil Engineering, Faculty of Engineering, University of Maragheh, Maragheh, Iran. Email: daneshfaraz@maragheh.ac.ir **(Corresponding Author)**

significant issues in hydraulic engineering and it helps engineers to design the structure and know the flow condition. So that the velocity of the flow entering the channels leads to the destruction of the foundation and bottom of the channel downstream of the bed by producing oscillating waves; therefore, it is necessary to design stilling basins in such a way dissipated flow energy and the depth of the downstream channel does not become less than the sequent depth. In irrigation networks, a large number of sluice gates are used. Considering the cost of their construction, if its dimensions can be chosen as small, it is effective in reducing the channel cost. One of the solutions, to reduce the dimensions of the gate, is to use a sill on the bottom of the channel and install the gate on it. Sill will reduce the design height of the gates and reduce the force on the gate; therefore, the use of a combined gate-sill structure can be considered. In addition, in recent years, the use of sills is one of the new ways to reduce the costs related to the construction of stilling basins.

So far, many analytical and experimental studies have been conducted to determine the hydraulic and geometric parameters of sluice gates [1-4]. Most of the studies carried out in sill mode have investigated the discharge coefficient of sluice gates such as Alhamid [5], Salmasi and Abraham [6], Ghorbani et al. [7], and Daneshfaraz et al. [8]. Among the studies conducted on the hydraulic jump downstream of the sluice gate, the following research can be mentioned:

Jalil et al. [9] evaluated the characteristics of hydraulic jumps downstream of sluice gates with sills. The results of their research showed that the presence of a sill under the sluice gate causes a 10% increase in energy dissipation. Abdelmonem et al. [10] investigated the energy dissipation downstream of the sluice gate using a pendulum sill installation. Using the pendulum sill as an energy dissipator increases the hydraulic jump efficiency by 20%. Habibzadeh et al. [11] investigated the hydraulic jump characteristics after the gate and reported the increase in water level fluctuations with the increase in Froude number. Ghaderi et al. [12] numerically investigated the hydraulic jump downstream of the gate with different forms of roughness in various placement arrangements. Their results showed that the thickness of the boundary layer in hydraulic jump decreases with the increase of the distance between roughness's.

The background of the research showed that in the studies conducted, the effect of suppressed and non-suppressed sills in different positions relative to the sluice gate has not been investigated on the parameters of the hydraulic jump downstream of the sluice gate. Considering that suppressed and non-suppressed sills and their position changes the hydraulic characteristics of the flow upstream and downstream of the gate, including the upstream depth, the initial depth, the sequent depth of hydraulic jump, streamlines of flow, parameters of hydraulic jump and energy dissipation, it is necessary to investigate these variables. Therefore, in the present study, the sills in different positions in single, double, and triple arrangements were investigated experimentally.

## 2. Materials and Methods
2.1. Experimental equipment
The experiments were done in the hydraulic laboratory of the University of Maragheh. Experiments have been performed on an open metal channel with a length of 5 meters, a width of 0.3 meters, and a depth of 0.45 meters. The walls of the channel are made of Plexiglas. In addition, screen plates were used at the beginning of the flume to reduce the turbulence of the inlet water. The slope of the channel was set to zero degrees for the experiments. Two pumps, each with a capacity of 0.0075 m^3/s, provide the flow rate. The flow rate has been measured through two Rotameters with a relative error of ±2% installed in the outlet of the pumps. A point gauge with an accuracy of ±1 mm has been used. In each series of experiments, after establishing the flow inside the flume, the depths were measured at the initial and sequent depths of the hydraulic jump. To reduce errors and increase measurement accuracy, the depths were measured at 4 points of the

cross-section, and their average was recorded as the final depth. The experiments have been carried out in the discharge range of 0.0025 to 0.0142 m³/s. In the present study, sills were investigated as the main parameter of the experiment. The dimensions of the sills were 0.05 m thickness, 0.03 m height, and 0.025, 0.05, 0.075, 0.10, 0.15, 0.20, 0.25, and 0.30 m widths. Figure (1) shows a view of the experimental flume.

(a)
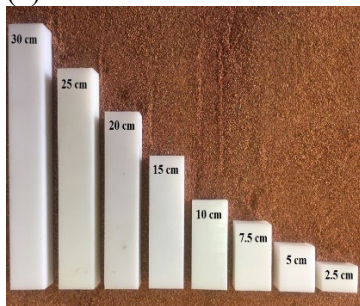
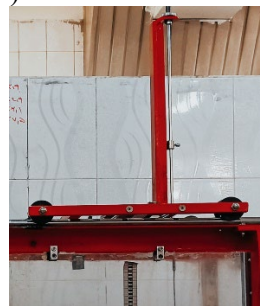(b)   (c)   (d)

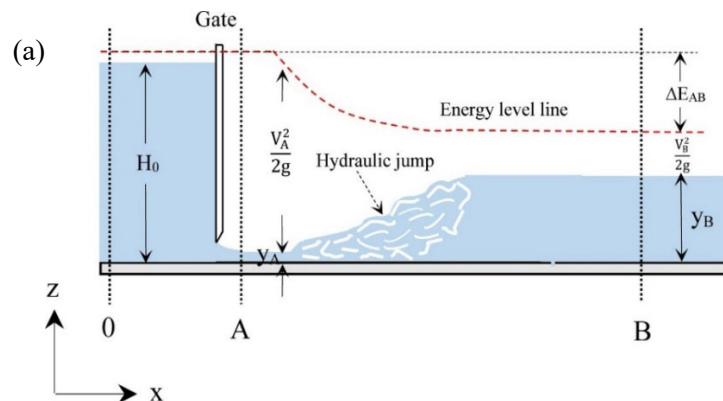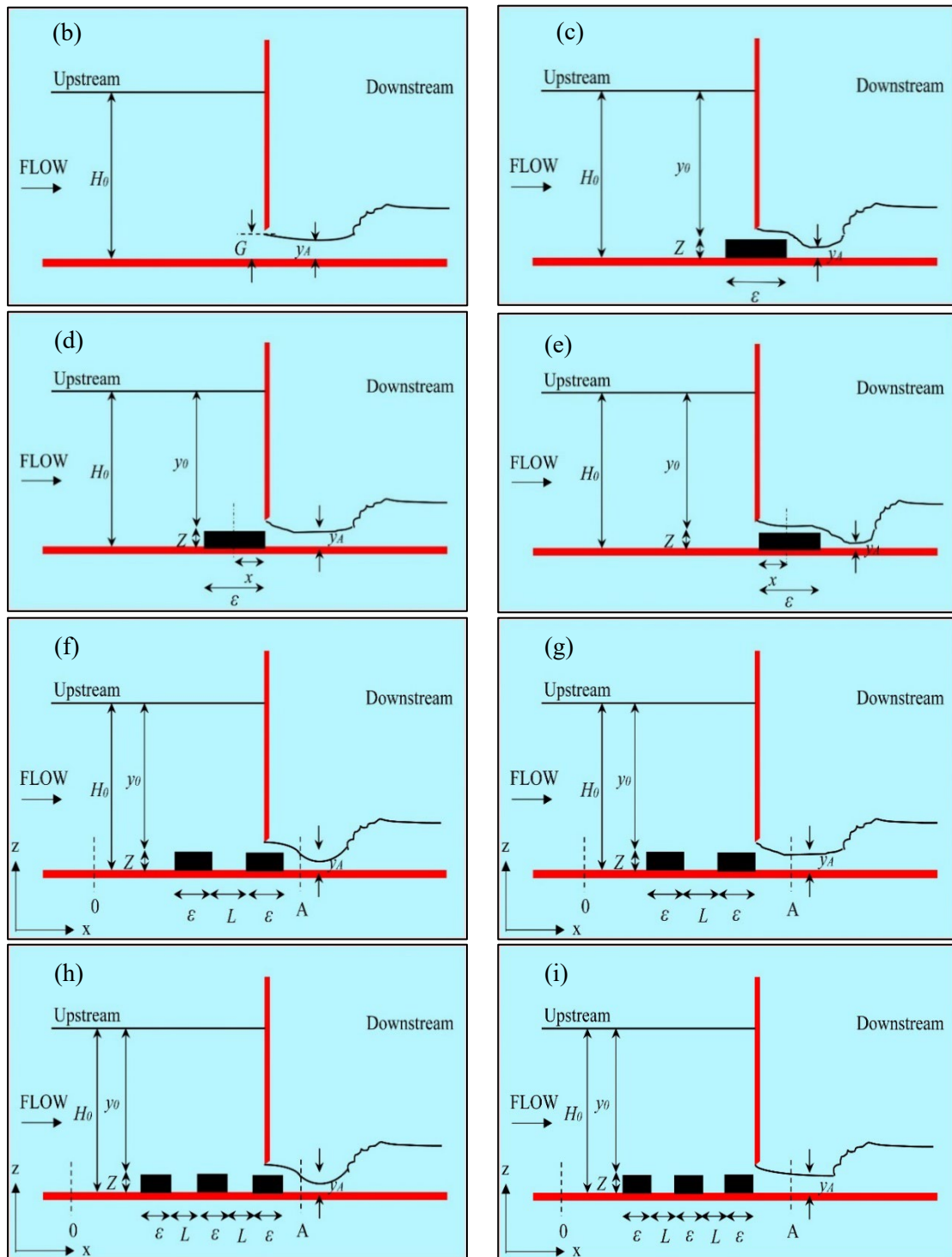**Figure 1. a) view of experimental flume b) physical model of sills c) point depth gauge d) pump, Rotameters, and panel box**

In Figure (2), the parameters related to the hydraulic jump, the positions of the sill relative to the sluice gate, and the hydraulic and geometric parameters of the sills are shown.
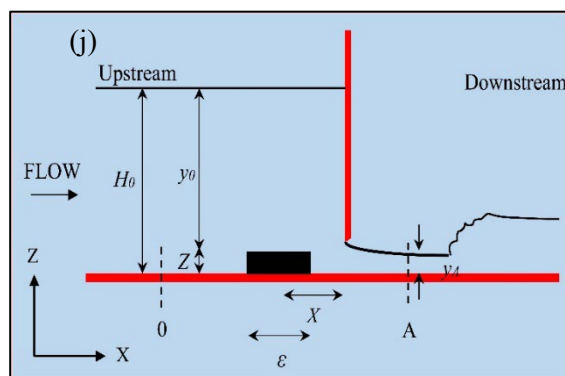
Figure 2. a) parameters of a hydraulic jump [13-14], the position of the sills relative to the sluice gate b) no-sill c, f, h) under the gate in the case of single, double, and triple sills, respectively, d, g, i) tangent position upstream of the gate in the case of single, double and triple sills, respectively, e) tangent position downstream of the gate, j) upstream of the gate at different distances relative to the gate

In Figure (2), H_0 is the upstream depth of the gate, y_0 is the flow depth above the sill, Z is the sill height, ε is the sill thickness, L is the distance between the sills, X is the axis-to-axis distance of the gate to the sill, y_A and y_B, are the flow depths in sections A and B, respectively.

2.2. Relations

$$E_A = \left(y_A + \frac{V_A^2}{2g} \right) \tag{1}$$

$$E_B = \left(y_B + \frac{V_B^2}{2g} \right) \tag{2}$$

$$Fr_A = \frac{V_A}{\sqrt{gD_A}} \tag{3}$$

In the above relations, E_A and E_B are the specific energy in sections A and B, respectively, V_A and V_B are the flow velocity in sections A and B, respectively, g is the gravitational acceleration, Fr_A represents the Froude number in section A, D_A is the hydraulic depth in section A which is equal to y_A in the rectangular channel. When the liquid is the same and the temperature is constant, in the experimental set-up, Reynolds number and Weber number are dependent on each other and vary with the opening of the gate, so one of the two must be eliminated, therefore the effect of Weber number was ignored [15-17]. Here, the flow is turbulent, so the effect of this parameter can be ignored [18-19].

2.3. Statistical indicators

In this research, statistical indicators of Absolute Error (AE), percentage Relative Error (RE%), Root Mean Square Error (RMSE) and Kling Gupta Efficiency (KGE) were used to investigate the performance of the presented equations and compare its results with experimental results.

$$AE = |x_{Obs} - x_{Cal}| \tag{4}$$

$$RE\% = \left|\frac{x_{Obs} - x_{Cal}}{x_{Obs}}\right| \times 100 \tag{5}$$

$$RMSE = \sqrt{\frac{\sum_{i=1}^{n}(x_{Obs} - x_{Cal})_i^2}{n}} \tag{6}$$

$$KGE = 1 - \sqrt{(R-1)^2 + (\beta-1)^2 + (\gamma-1)^2}$$

$0,7 < KGE < 1 \ Very \ good$

$0,6 < KGE < 0,7 \ Good$

$$\beta = \frac{\overline{x_{Cal}}}{\overline{x_{Obs}}} . \gamma = \frac{CV_{Cal}}{CV_{Obs}} = \frac{\sigma_{Cal}/\overline{x_{Cal}}}{\sigma_{Cal}/\overline{x_{Obs}}}$$

$0,5 < KGE \le 0,6 \ Satisfactory$ $\tag{7}$

$$R = \frac{[\sum_{i=1}^{n}(x_{Obs\ i} - \overline{x_{Obs}}) \times (x_{Cal\ i} - \overline{x_{Cal}})]}{\sum_{i=1}^{n}(x_{Obs\ i} - \overline{x_{Obs}})\sum_{i=1}^{n}(x_{Cal\ i} - \overline{x_{Cal}})}$$

$0,4 < KGE \le 0,5 \ Acceptable$

$KGE \le 0,4 \ Unsatisfactory$

In the above relationships, *n* is the total number of data, Obs and Cal represent observation and calculation results, respectively. The values of relationships (4, 5, and 6), as close as they are to zero, indicate the high accuracy of the presented equations. In relation (7), R is the correlation coefficient, β is the ratio of average calculated data to average observed data, and γ is the ratio of the standard deviation of the calculated values to the standard deviation of the observed values. KGE statistical indicator based on the division of this index into very good, good, satisfactory, acceptable, and unsatisfactory, can indicate the accuracy of the presented equations [20].

3. Results and Discussion
3.1. Energy dissipation in the no-sill state

The examination of the experimental results has been done by two dimensionless parameters of the ratio of energy dissipation to the upstream and downstream specific energy of the hydraulic jump ($\Delta E_{AB}/E_A$ and $\Delta E_{AB}/E_B$). One of the most significant parameters to analysis energy dissipation is the Froude number (Fr_A). In Figures (3-a and b), the relative energy dissipation is presented, where the horizontal axis is the dimensionless parameter Fr_A, and the vertical axis represents the ratio of the energy dissipation to the specific energy of the flow in sections A and B. The relative energy dissipation is increasing with a certain trend with increasing Froude number. The reason for the convexity and concavity of the curve can be related to the flow regime in sections A and B, so that the flow in section A is supercritical and in section B is subcritical, which leads to the high specific energy in section A compared to the specific energy in section B. The amount of energy dissipation in different discharges and openings is given in Figures (3-c and d). The relative energy dissipation is the lowest at a 5 cm opening, and the relative energy dissipation has increased with the decrease of the gate opening. So that by increasing the gate opening, the velocity of the flow through the gate decreases, and the initial depth of the flow increases, which in itself causes a decrease in the specific energy in section A. An increase in the initial depth leads to a decrease in the sequent depth compared to smaller openings. As a result, the specific energy in section B decreases as in section A; therefore, the specific energy difference between sections A and B will be small. According to Figures (3-c and d), in constant discharge, the amount of relative energy dissipation in the opening of 1 cm is higher than the opening of 2,

4, and 5 cm, respectively. Therefore, the average ratio of energy dissipation to the upstream specific energy in the opening of 1 cm is 21.01%, 58.38%, and 63.54% more than the opening of 2, 4, and 5 cm, respectively. Meanwhile, this amount for downstream is 55.41%, 87.08%, and 89.54%, respectively.
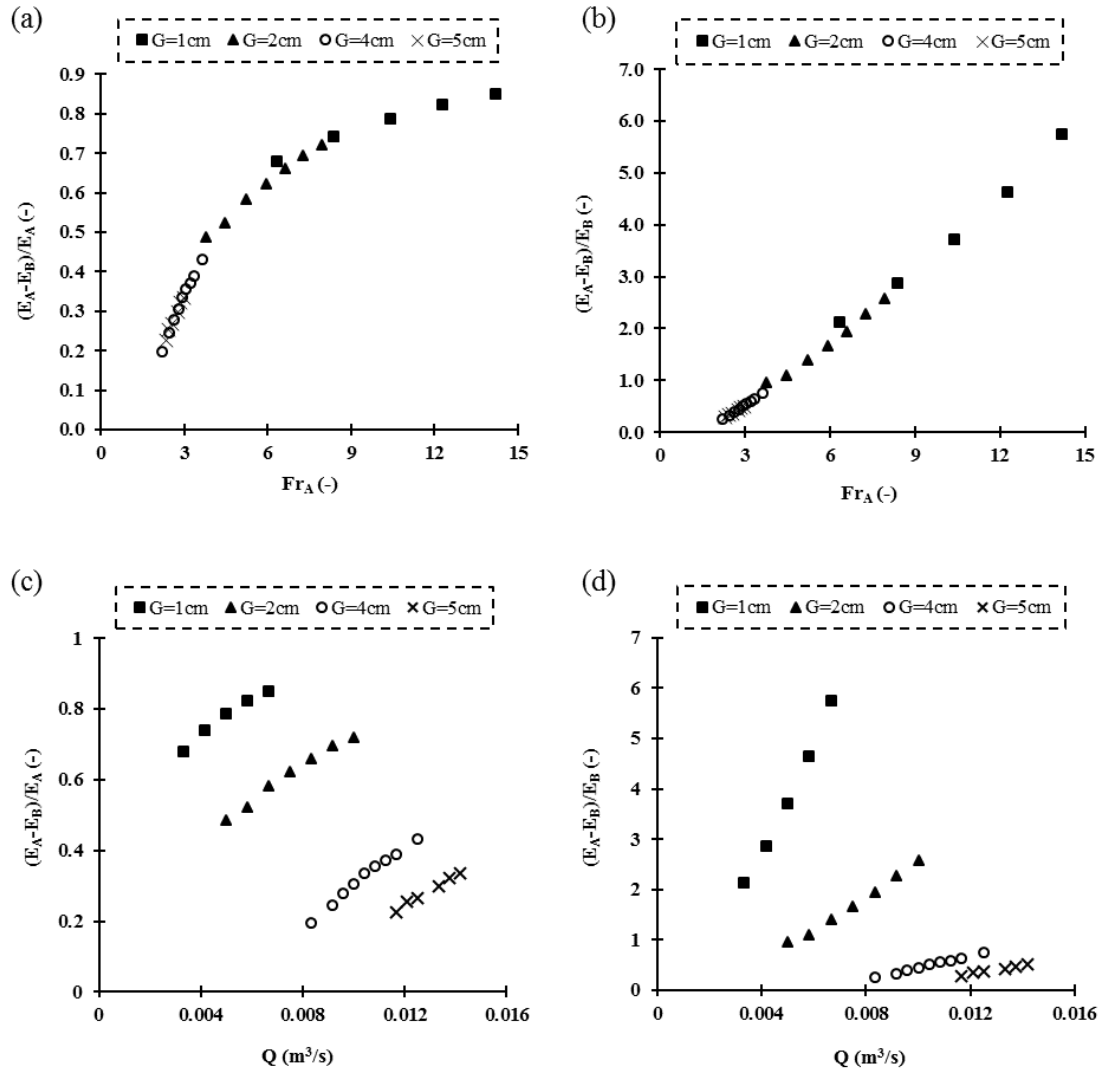
Figure 3. Relative energy dissipation in different gate openings

3.2. The relative depth of the hydraulic jump in the no-sill state

The relative depth of the hydraulic jump (y_B/y_A) is a function of the Froude number in section A (Fr_A). The diagram of the relative depth of the hydraulic jump is shown against the Fr_A for all openings (Figure 4-a). The relative depth of the hydraulic jump increases linearly between the data with the increase of the Fr_A. The reason for this is the significant effect of gate opening on sequent depth increase. At the same discharge, the sequent depth is greater than the gate with a larger gate opening. According to Figures (4-a and b), the hydraulic jump is classified into different types

according to the Fr_A. In addition, the strength and intensity of the hydraulic jump depend on the Fr_A. As the Fr_A increases, the ratio of the sequent depth to the initial depth (y_B/y_A); in other words, the wave height (y_B-y_A) increases. The direct relationship of energy dissipation with the third power of the expression (y_B-y_A) makes the amount of energy dissipation highly sensitive to the intensity of the hydraulic jump.

(a)

(b)

Figure 4. a) Changes of relative depth versus the Froude number b) Formation of different types of hydraulic jumps according to the various Froude number

One of the basic parameters in the design of hydraulic structures is the length of the hydraulic jump. The hydraulic jump length is mea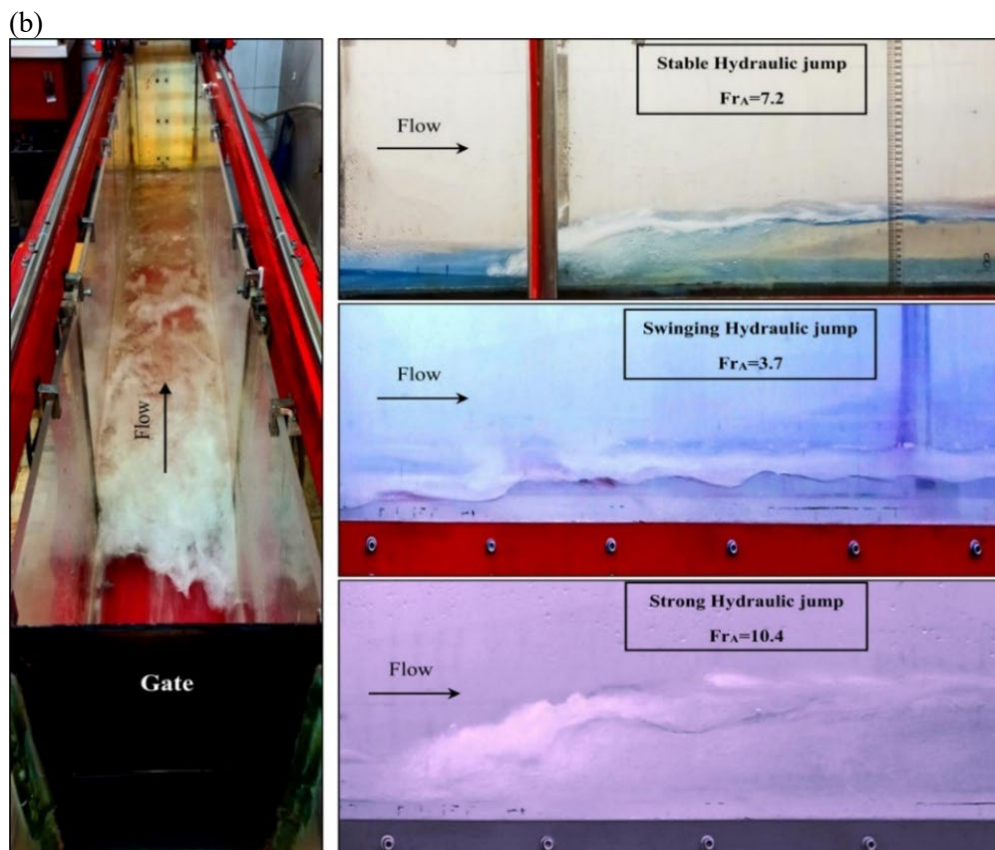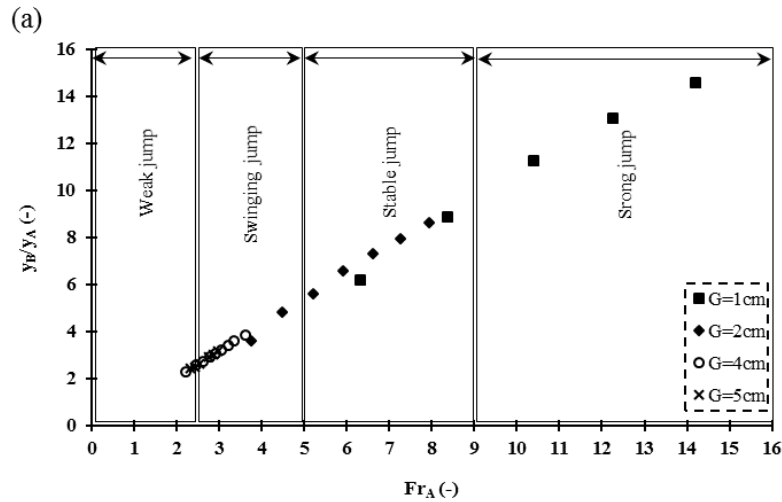sured as the distance between the beginning of the hydraulic jump and the last wave of the eddy current. In Figure (5-a), the ratio of hydraulic jump length to the initial depth of the jump is drawn for all gate openings in different Froude numbers. In addition, in Figure (5-b), the ratio of the jump length curve to the sequent depth is shown. As can be seen, the length of the jump increases with the increase of the Froude number. In other words, increasing the Froude number leads to increasing turbulence and eddy currents at the start of the hydraulic jump.
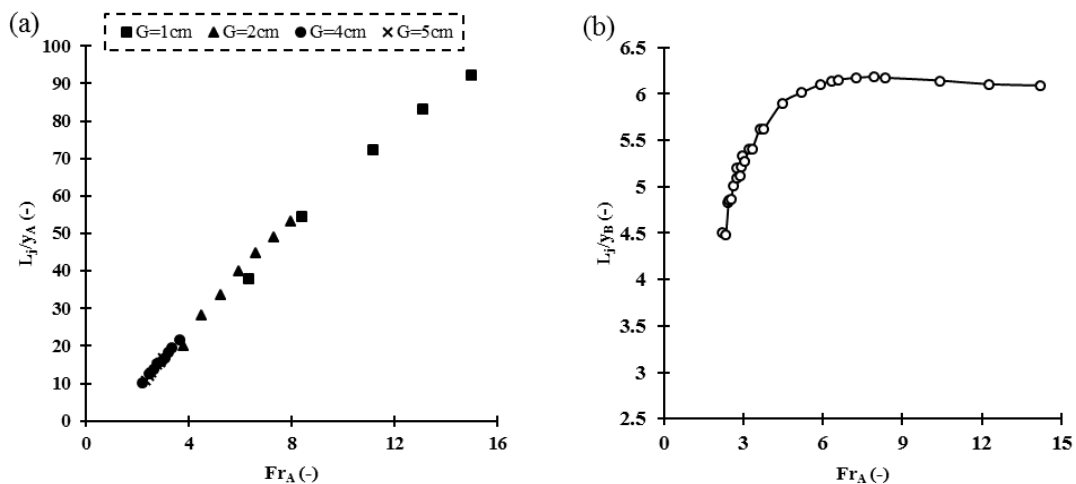
Figure 5. Relative length of the hydraulic jump to the a) initial depth b) sequent depth of the hydraulic jump

3.3. Investigating specific energy versus depth in the sill state

In Figure (6), the values of specific energy in sections A and B against the corresponding depths are drawn in the positions below and tangent to the gate upstream and downstream. According to the results obtained in Figure (6) with the increase of y, the height equivalent to the velocity ($V^2/2g$) is reduced, and with the decrease of y, the height equivalent to the velocity is increased. Carefully in Figure (6), we can conclude that for a constant discharge, there are two positive answers for the specific energy equation (E), which is the supercritical flow for $y_A < y_{critical}$ state and subcritical flow for $y_B > y_{critical}$ state. According to Figure (6), in the supercritical flow, with the increase of specific energy, the depth of flow decreases, and in the case of subcritical flow, with the increase of specific energy, the depth of the flow increases.
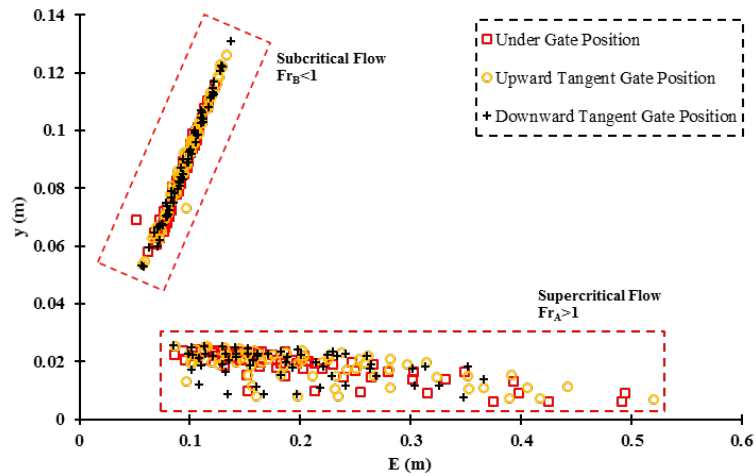
Figure 6. specific energy against depth

3.4. Relative energy dissipation ($\Delta E_{AB}/E_A$ and $\Delta E_{AB}/E_B$) versus the Froude number (Fr_A) in the sill state

In this section, sills are placed in total openings of 4 and 5 cm. The amount of relative energy dissipation of all studied sill widths for various positions of the sill relative to the gate is shown in Figure (7). It should be noted that the results of different widths of 2.5, 5, 7.5, 10, 15, 20, 25, and 30 cm for the sill positions are combined and shown in the form of a specific legend for each position. With the increase of the Froude number, the amount of energy dissipation increases with a certain convex and concave trend. For the total opening of 5 cm, sill widths of 5, 10, 20 and 30 cm have been investigated. Considering that the experiments for each model were carried out in a specific range of discharge; therefore the range of Froude number changes in Figures (7-c and d) is smaller compared to Figures (7-a and b) due to the gate opening.

(a)   (b)

(c)

(d)
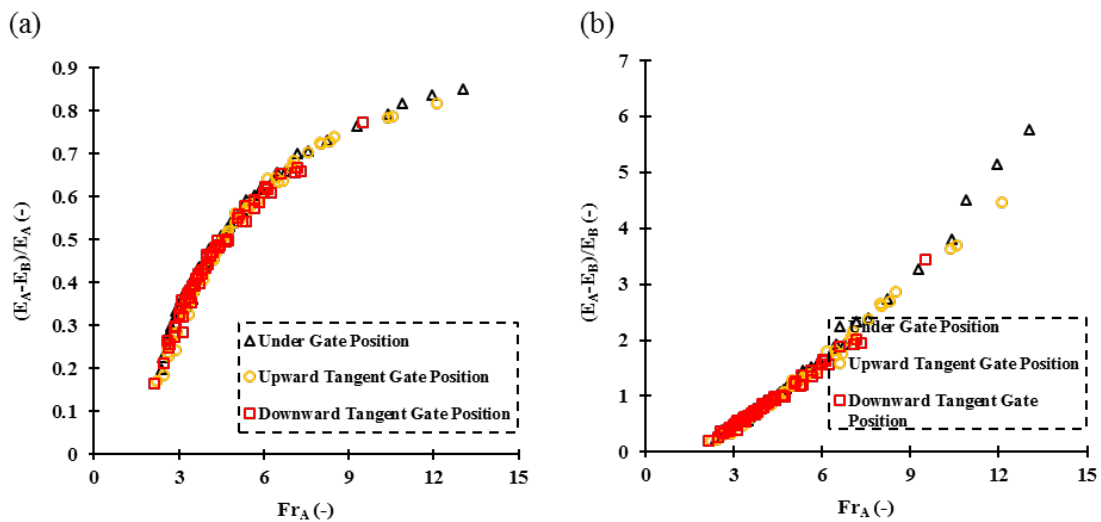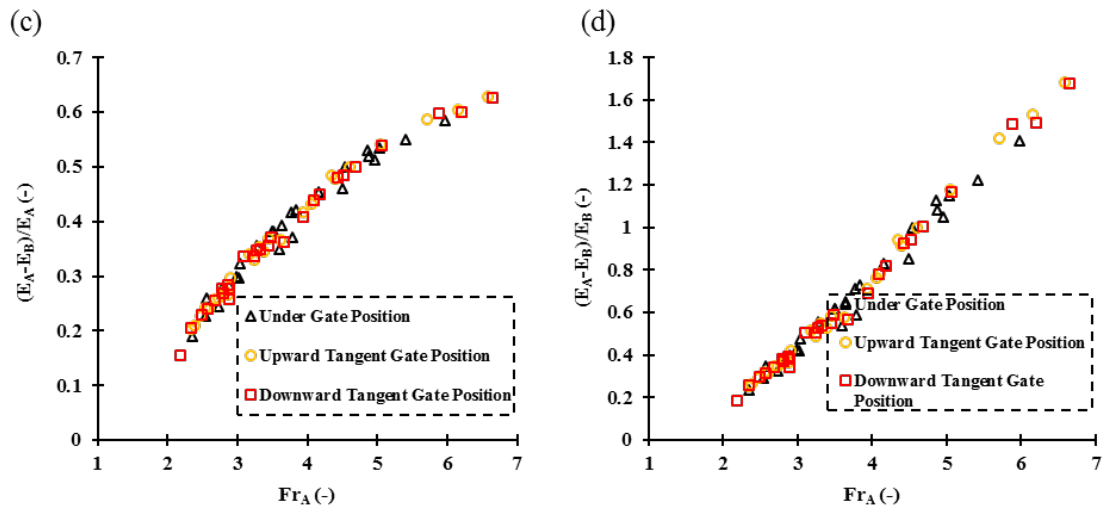
Figure 7. Ratio of energy dissipation to a-c) upstream specific energy of the hydraulic jump b-d) downstream specific energy of the hydraulic jump versus Froude number in the opening a-b) 4 cm c-d) 5 cm

3.5. Relative energy dissipation ($\Delta E_{AB}/y_A$) versus relative depth (y_A/y_B) in the sill state

Figures (8-a and b) show the relationship between the ratio of energy dissipation to the initial depth ($\Delta E_{AB}/y_A$) and the relative depth (y_A/y_B) for the total opening of 4 and 5 cm, respectively. As the y_A/y_B increases, the value of $\Delta E_{AB}/y_A$ decreases with a clear trend and a high determination coefficient. This happens due to the convergence of the initial and sequent depths, so that increasing the initial depth leads to the formation of a weak jump and low energy dissipation. In addition, the increase in y_A decreases the Froude number, and consequently, the energy dissipation decreases. According to Figure (8), the highest amount of energy dissipation is related to the ratio $y_A/y_B=0.1$. In other words, in a constant discharge, with the increase of the sill, the initial depth decreases, and consequently, the sequent depth increases; so the energy loss increases, which the ratio $y_A/y_B=0.1$ shows this.

(a)
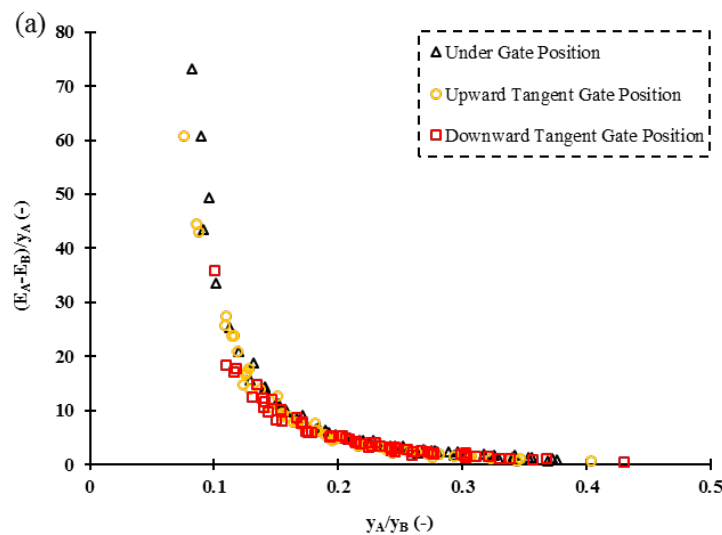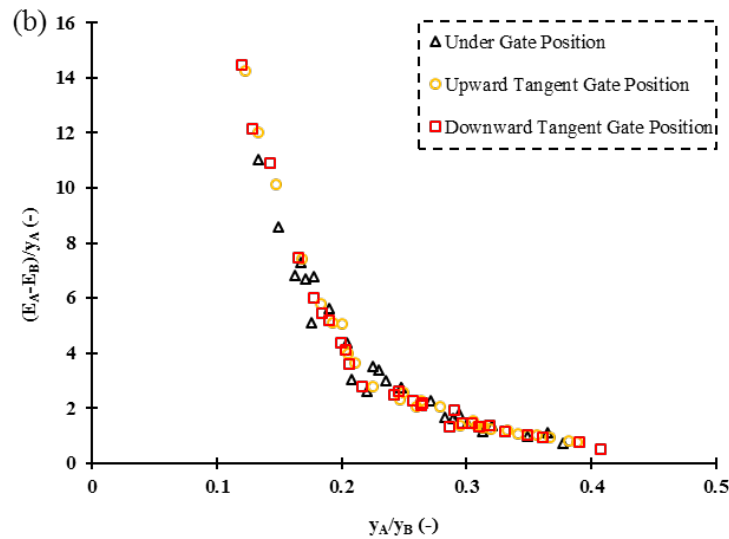
Figure 8. The relationship between $\Delta E_{AB}/y_A$ and y_A/y_B for different positions of the sill relative to the sluice gate in the opening a) 4 cm b) 5 cm

3.6. Relative energy dissipation ($\Delta E_{AB}/E_A$ and $\Delta E_{AB}/E_B$) at different sill positions

The energy dissipation relative to the upstream and downstream specific energy of the hydraulic jump in different discharges for all the studied widths in the opening of 4 cm of the valve is presented in Figure (9). According to Figure (9), it can be seen that with the increase of sill width, the amount of relative energy dissipation increases. Increasing the width causes the flow to pass uniformly under the gate, and in addition, it leads to a decrease in the gate opening, which itself leads to a decrease in the initial depth of the hydraulic jump. Also, by comparing the amount of relative energy dissipation in all three positions, the under gate one has more energy dissipation than other sill positions. On average, by comparing Figures (9-a, b, and c) with each other, the ratio of energy dissipation to the upstream and downstream specific energy in the under gate state in all the studied widths from small to large is 13.69%, 2.71%, %, 1.86%, 3.63%, 4.97%, 8.81%, 15.08%, and 11.05% are more than the upstream tangential state, respectively. Also, these values are 13.05%, 0.16%, 8.88%, 5.86%, 10.23%, 10.82%, 17.65%, and 14.56% more than the downstream tangential state, respectively. In addition, this comparison was made for the relative energy dissipation in Figures (9-d, e, and f) with each other. The relative energy dissipation in the under gate state is 18.59%, 5.05%, 4.25%, 11.68%, 6.50%, 21.66%, 33.99%, and 28.71% more than the upstream tangential state, respectively. The position under the gate compared to the downstream tangential position is 17.72%, 0.80%, 15.79%, 8.82%, 21.02%, 22.18%, 49.97%, and 48.23%, respectively.

(f)
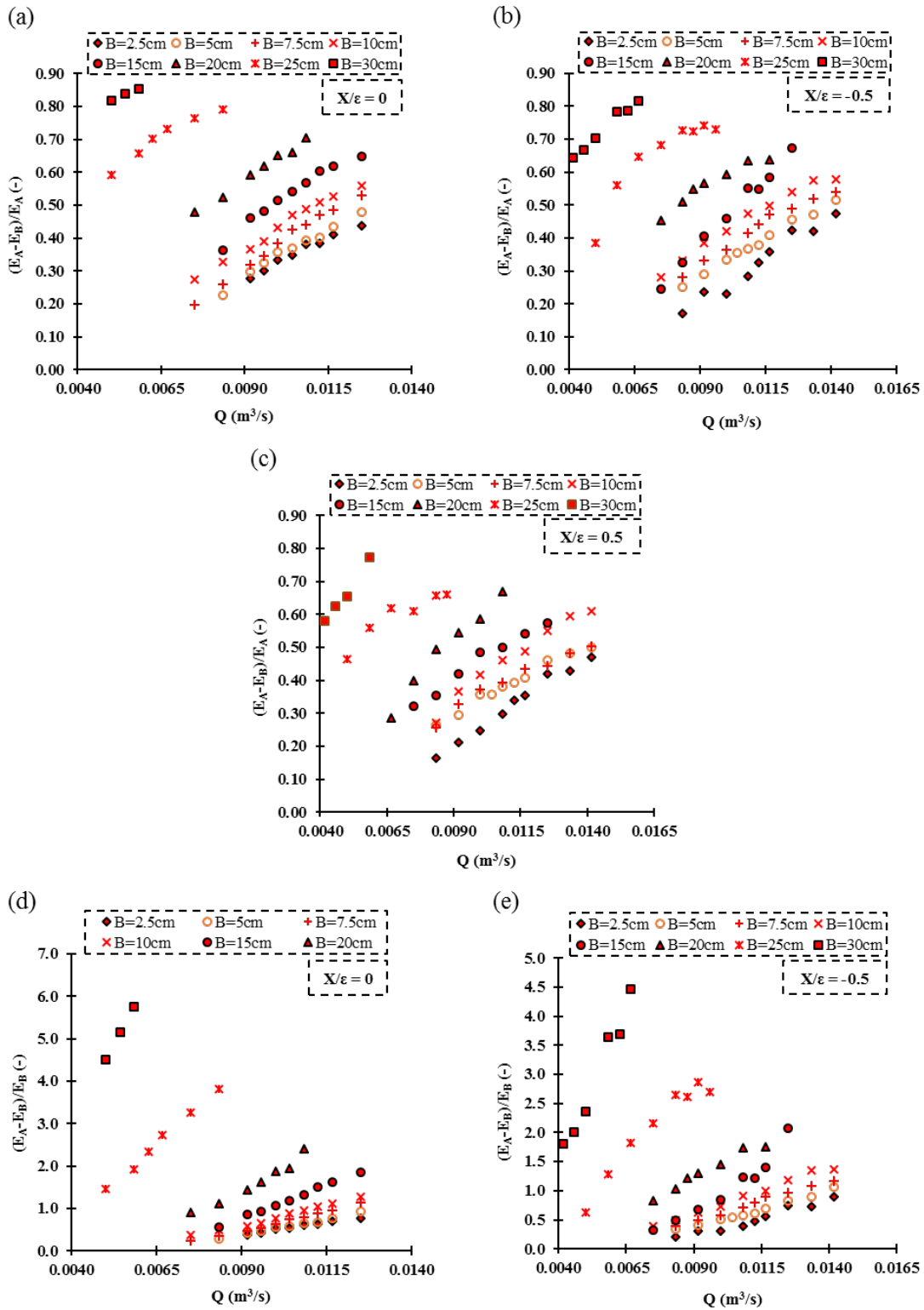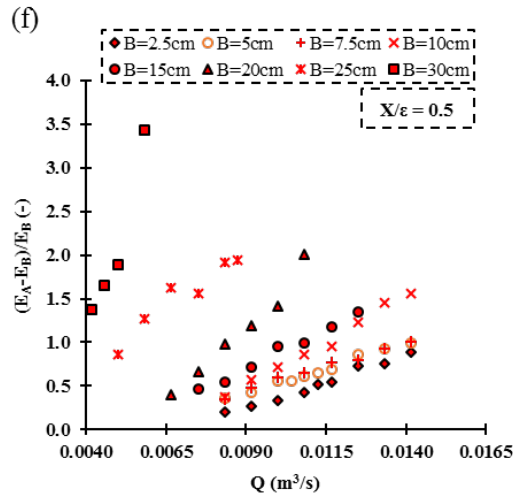
Figure 9. (total gate opening = 4 cm). The amount of energy dissipation in the sill state a, d) under the gate mode b, e) upstream tangential mode c, f) downstream tangential state compared to a, b, c) upstream specific energy d, e, f) downstream special energy

In Figure (10), the studied sills are placed under a total opening of 5 cm. The results of the energy dissipation relative to the upstream and downstream specific energy of the hydraulic jump at different discharges are shown in this figure. The amount of relative energy dissipation is lower compared to the smaller gate opening presented in Figure (10). The cause of this issue can be related to the gate opening, which leads to the change of conditions in the relative depths and the type of hydraulic jump formation.

(a)

(b)

(c)

(d)

(e)

(f)
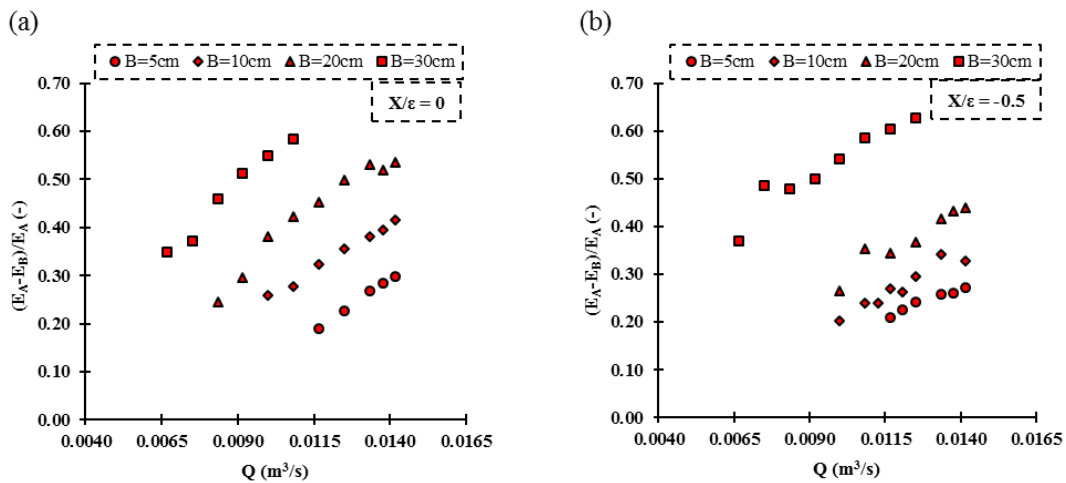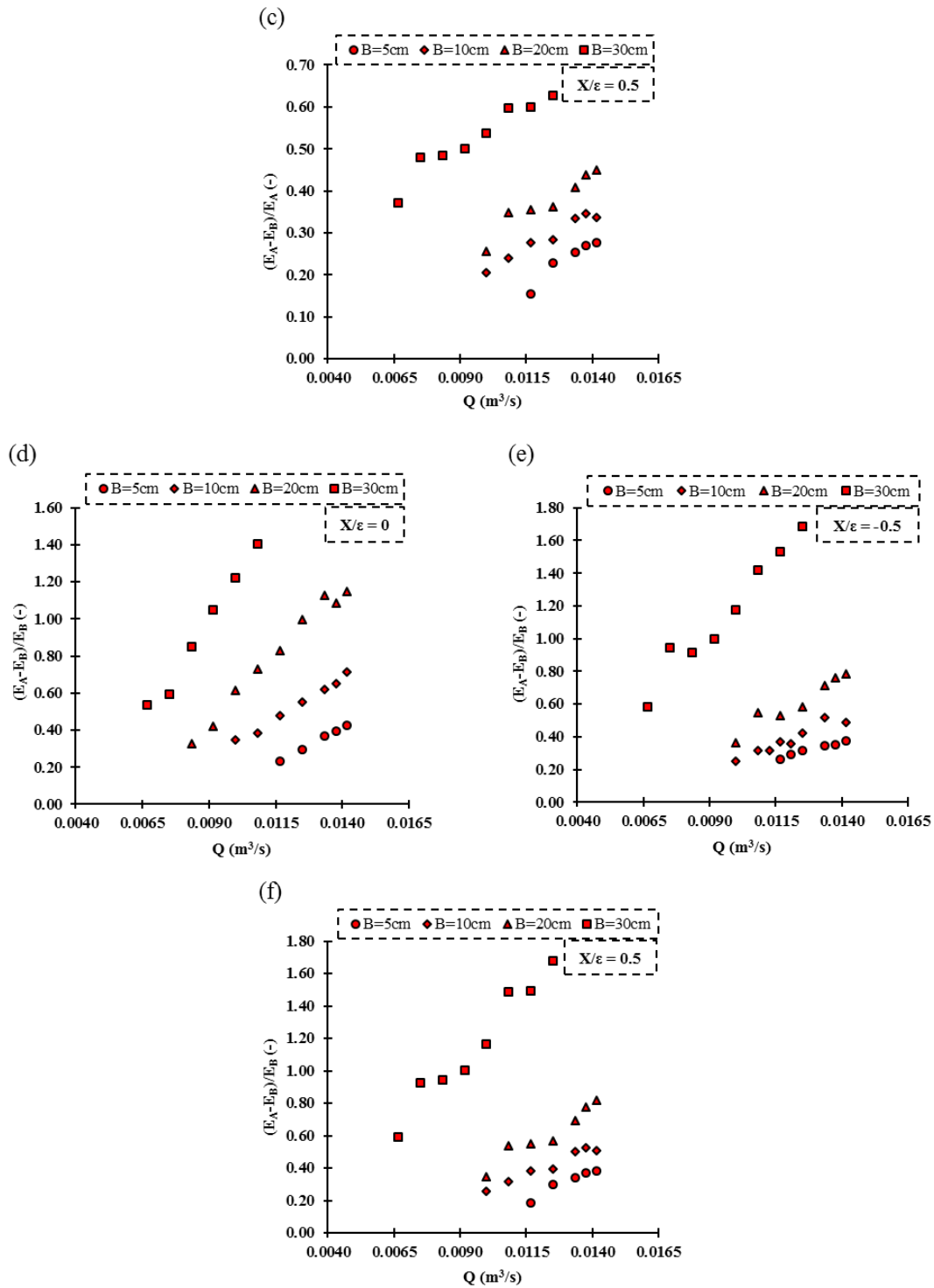
Figure 10. (total gate opening = 5 cm). The amount of energy dissipation in the sill state a, d) under the gate mode b, e) upstream tangential mode c, f) downstream tangential mode compared to a, b, c) upstream specific energy d, e, f) downstream special energy

3.7. Comparison of the sequent depth in the no-sill and with the sill in the same opening

In this section, the sequent depth of the hydraulic jump was investigated in the case of no-sill and with the suppressed sill in the openings of 1 and 2 cm in different positions of the sill under the gate and tangent to the gate upstream and downstream. The use of a sill in all placement conditions relative to the gate leads to a decrease in the sequent depth compared to the no-sill state (Table 1). Reducing the sequent depth and specific energy reduces the height of the channel walls and is economically viable. In addition, due to the supercritical flow condition at the initial depth, the decrease in the depth of the flow leads to an increase in the specific energy in that section, which in turn causes an increase in the velocity of the passing flow and flooring and causing damage to the channel bottom. Therefore, a way that can reduce the specific energy at the initial depth of the hydraulic jump can prevent damage to facilities and channels. The application of suppressed compared to the no-sill state increases the initial depth and consequently the initial specific energy decreases (Table 2). The use of the sill leads to the reduction of the specific energy in the depth of the flow conjugate, which can be of interest to engineers and users.

Table 1. The sequent depth of the hydraulic jump in the no-sill and with a sill state in different placement positions

Q (m³/s)	Gate opening=1 cm			
	Sequent depth (m)			
	No Sill	$X/\varepsilon=0$	$X/\varepsilon=-0.5$	$X/\varepsilon=0.5$
0.0033	0.042	-	-	-
0.0042	0.058	-	0.053	0.053
0.0046	-	-	0.063	0.059
0.0050	0.072	0.065	0.067	0.065
0.0054	-	0.069	-	-
0.0058	0.083	0.074	0.081	0.075
0.0063	-	-	0.086	-
0.0067	0.092	-	0.092	-

Q (m³/s)	Gate opening=2 cm			
	Sequent depth (m)			
	No Sill	$X/\varepsilon=0$	$X/\varepsilon=-0.5$	$X/\varepsilon=0.5$
0.0050	0.045	-	-	-
0.0058	0.060	-	-	-
0.0067	0.069	0.070	0.065	0.066
0.0075	0.080	0.079	0.075	0.078
0.0083	0.089	0.088	0.083	0.085
0.0092	0.097	0.097	0.090	0.092
0.0100	0.105	0.105	0.098	0.099
0.0110	-	0.117	0.109	0.110
0.0117	-	-	0.120	0.124
0.0125	-	-	0.130	0.132

Table 2. Specific energy of section A in the no-sill and with a sill state in different placement positions

Q (m³/s)	Gate opening=1 cm			
	Specific energy of section A (m)			
	No Sill	X/ε=0	X/ε=-0.5	X/ε=0.5
0.0033	0.143	-	-	-
0.0042	0.236	-	0.160	0.134
0.0046	-	-	0.198	0.167
0.0050	0.387	0.375	0.235	0.197
0.0054	-	0.425	-	-
0.0058	0.527	0.492	0.389	0.348
0.0063	-	-	0.417	-
0.0067	0.689	-	0.521	-

Q (m³/s)	Gate opening=2 cm			
	Specific energy of section A (m)			
	No Sill	X/ε=0	X/ε=-0.5	X/ε=0.5
0.0050	0.102	-	-	-
0.0058	0.137	-	-	-
0.0067	0.179	0.118	0.112	0.113
0.0075	0.226	0.134	0.157	0.160
0.0083	0.277	0.175	0.170	0.176
0.0092	0.333	0.209	0.191	0.195
0.0100	0.395	0.245	0.226	0.227
0.0108	-	0.292	0.276	0.286
0.0117	-	-	0.318	0.322
0.0125	-	-	0.363	0.367

3.8. Investigating parameters of hydraulic jump with the single sill in upstream positions of the gate

Single sills are placed at specified intervals of 7.5 and 17.5 cm upstream of the gate. The gate opening for all models is 4 cm. For the distance of 7.5 cm, all widths of the sill have been examined, while at the distance of 17.5 cm, due to the fact that the flow does not engage with the gate and the critical flow on the sill is created in the sill with larger widths, the widths 2.5, 5, 7.5 and 10 cm were investigated. Tables (3 and 4) show the effect of sill placement distance upstream of the sluice gate on the specific energy of the hydraulic jump in sections A and B. In these models, the gate is in a no-sill mode and the sills are located at a certain distance from the valve, so they do not affect the area of the flow through the gate. However, at X=7.5 cm, the increase in the width of the sill leads to an increase in the fluid depth upstream of the gate, and accordingly, the upstream pressure increases, so the flow exiting the gate has a high velocity and the depth is relatively reduced compared to the no-sill state. As a result, the specific energy in section A increases. Hydraulic parameters in section B have changed based on the change of flow characteristics in section A, so that; it increases the sequent depth and specific energy in section B (Table 3). The changes mentioned in X=17.5 cm were not like this and due to its large distance from the gate, not many changes are observed and the results are close to the no-sill state (Table 4).

Table 3. The specific energy of the hydraulic jump of sections A and B in with sill state at a distance of 7.5 cm upstream of the gate

X=7.5 cm

Q(m³/s)	No-Sill		B=2.5 cm		B=5 cm		B=7.5 cm		B=10 cm		B=15 cm		B=20 cm		B=25 cm		B=30 cm	
	E_A	E_B	E_A	E_B	E_A	E_B	E_A	E_B	E_A	E_B	E_A	E_B	E_A	E_B	E_A	E_B	E_A	E_B
0.0083	0.087	0.070	0.086	0.071	0.087	0.072	0.089	0.072	0.087	0.072	0.089	0.072	0.094	0.073	0.100	0.075	0.101	0.075
0.0092	0.101	0.076	0.100	0.078	0.101	0.079	0.101	0.078	0.109	0.079	0.104	0.081	0.110	0.080	0.112	0.083	0.118	0.083
0.0096	0.110	0.079	0.107	0.081	0.108	0.082	0.108	0.082	0.109	0.083	0.112	0.085	0.118	0.084	0.122	0.087	0.127	0.087
0.0100	0.116	0.083	0.115	0.085	0.115	0.085	0.118	0.086	0.116	0.086	0.121	0.089	0.126	0.089	0.134	0.092	0.137	0.092
0.0104	0.128	0.085	-	-	-	-	-	-	-	-	-	-	-	-	-	-	-	-
0.0108	0.133	0.089	0.131	0.092	0.131	0.093	0.134	0.094	0.134	0.093	0.139	0.096	0.146	0.096	0.151	0.098	0.158	0.098
0.0113	0.148	0.093	-	-	-	-	-	-	-	-	-	-	-	-	-	-	-	-
0.0117	0.153	0.096	0.149	0.100	0.149	0.099	0.153	0.100	0.155	0.100	0.159	0.102	0.166	0.102	0.171	0.104	0.176	0.104
0.0125	0.170	0.102	0.169	0.107	0.169	0.107	0.171	0.108	0.170	0.110	0.179	0.110	0.189	0.110	0.194	0.110	0.206	0.110
0.0133	-	-	0.190	0.116	0.192	0.114	0.196	0.115	0.194	0.115	0.200	0.116	0.209	0.118	0.220	0.121	0.233	0.121
0.0142	-	-	0.216	0.122	0.217	0.122	0.222	0.123	0.220	0.123	0.224	0.123	0.237	0.126	0.244	0.127	0.273	0.127

Table 4. The specific energy of the hydraulic jump of sections A and B in with sill state at a distance of 17.5 cm upstream of the

X=17.5 cm

Q(m³/s)	No-Sill		B=2.5 cm		B=5 cm		B=7.5 cm		B=10 cm	
	E_A	E_B	E_A	E_B	E_A	E_B	E_A	E_B	E_A	E_B
0.0083	0.087	0.070	0.085	0.071	0.086	0.071	0.086	0.071	0.086	0.072
0.0092	0.101	0.076	0.098	0.078	0.099	0.078	0.099	0.078	0.099	0.078
0.0096	0.110	0.079	0.105	0.081	0.106	0.082	0.106	0.082	0.106	0.082
0.0100	0.116	0.083	0.113	0.084	0.114	0.085	0.114	0.085	0.114	0.085
0.0104	0.128	0.085	-	-	-	-	-	-	-	-
0.0108	0.133	0.089	0.128	0.092	0.131	0.092	0.130	0.093	0.129	0.093
0.0113	0.148	0.093	-	-	-	-	-	-	-	-
0.0117	0.152	0.096	0.146	0.101	0.148	0.100	0.145	0.100	0.148	0.101
0.0125	0.170	0.102	0.166	0.107	0.166	0.107	0.170	0.107	0.168	0.106
0.0133	-	-	0.185	0.115	0.190	0.115	0.191	0.114	0.187	0.114
0.0142	-	-	0.205	0.121	0.211	0.122	0.210	0.121	0.212	0.121

3.9. Comparison of hydraulic characteristics of hydraulic jump in single and double sill state

In Table (5), the hydraulic characteristics of the hydraulic jump, including the sequent depth and specific energy in section B for the single and double sill state are presented for the under gate sill position. According to Table (5), the sequent depth increases with the increase of discharge for single and double sill states, and its highest value is related to the double sill state. Considering the subcritical flow in section B, increasing the sequent depth increases the specific energy in section B. In Table (6), for the upstream tangential sill in the single and double state, the results are close to each other and the values of the double sill mode are slightly higher than the single sill mode.

Table 5. Comparison of depth and specific energy of section B in single and double sill state for under gate sill mode

Under gate sill mode

Q(m³/s)	B=2.5 cm Single sill y_B	E_B	Double sill y_B	E_B	B=5 cm Single sill y_B	E_B	Double sill y_B	E_B	B=7.5 cm Single sill y_B	E_B	Double sill y_B	E_B	B=10 cm Single sill y_B	E_B	Double sill y_B	E_B
0.0075	-	-	-	-	-	-	-	-	0.061	0.069	-	-	0.061	0.069	0.064	0.072
0.0083	-	-	-	-	0.063	0.073	0.066	0.075	0.067	0.076	0.067	0.076	0.068	0.077	0.070	0.078
0.0092	0.065	0.076	0.068	0.078	0.066	0.077	0.071	0.080	0.074	0.083	0.075	0.083	0.074	0.083	0.079	0.087
0.0096	0.068	0.079	-	-	0.071	0.081	-	-	0.081	0.089	-	-	0.081	0.089	-	-
0.0100	0.070	0.082	0.077	0.086	0.073	0.083	0.080	0.089	0.085	0.092	0.081	0.090	0.085	0.093	0.088	0.095
0.0104	0.078	0.088	-	-	0.079	0.089	-	-	0.086	0.094	-	-	0.088	0.096	-	-
0.0108	0.079	0.090	0.084	0.093	0.082	0.092	0.087	0.096	0.092	0.100	0.091	0.099	0.093	0.101	0.096	0.103
0.0113	0.085	0.095	-	-	0.088	0.097	-	-	0.094	0.102	-	-	0.097	0.105	-	-
0.0117	0.087	0.097	0.094	0.103	0.089	0.099	0.095	0.104	0.099	0.107	0.099	0.107	0.101	0.109	0.108	0.114
0.0125	0.095	0.105	0.100	0.109	0.097	0.106	0.104	0.112	0.108	0.116	0.107	0.115	0.110	0.117	0.115	0.121
0.0133	-	-	0.108	0.117	-	-	0.115	0.122	-	-	0.114	0.122	-	-	-	-
0.0142	-	-	-	-	-	-	0.122	0.128	-	-	0.123	0.130	-	-	-	-

Q(m³/s)	B=15 cm Single sill y_B	E_B	Double sill y_B	E_B	B=20 cm Single sill y_B	E_B	Double sill y_B	E_B	B=25 cm Single sill y_B	E_B	Double sill y_B	E_B	B=30 cm Single sill y_B	E_B	Double sill y_B	E_B
0.0038	-	-	-	-	-	-	-	-	-	-	-	-	-	-	0.052	0.055
0.0042	-	-	-	-	-	-	-	-	-	-	0.054	0.058	-	-	0.059	0.062
0.0050	-	-	-	-	-	-	-	-	0.058	0.062	0.065	0.068	0.065	0.068	0.070	0.073
0.0054	-	-	-	-	-	-	-	-	-	-	-	-	0.069	0.072	0.078	0.081
0.0058	-	-	0.055	0.061	-	-	0.065	0.069	0.069	0.073	0.078	0.081	0.074	0.078	-	-
0.0063	-	-	-	-	-	-	-	-	0.072	0.076	0.082	0.085	-	-	-	-
0.0067	-	-	0.063	0.070	-	-	0.074	0.079	0.081	0.084	0.091	0.094	-	-	-	-
0.0075	-	-	0.071	0.077	0.073	0.079	0.083	0.087	0.089	0.093	0.099	0.102	-	-	-	-
0.0079	-	-	-	-	-	-	-	-	-	-	0.104	0.107	-	-	-	-
0.0083	0.077	0.084	0.082	0.088	0.083	0.088	0.091	0.096	0.099	0.103	-	-	-	-	-	-
0.0092	0.081	0.088	0.089	0.095	0.092	0.098	0.099	0.104	-	-	-	-	-	-	-	-
0.0096	0.085	0.092	-	-	0.095	0.101	-	-	-	-	-	-	-	-	-	-
0.0100	0.091	0.098	0.098	0.104	0.099	0.105	0.109	0.114	-	-	-	-	-	-	-	-
0.0104	0.094	0.101	-	-	0.108	0.113	-	-	-	-	-	-	-	-	-	-
0.0108	0.101	0.108	0.108	0.114	0.110	0.116	0.120	0.124	-	-	-	-	-	-	-	-
0.0113	0.105	0.111	-	-	-	-	-	-	-	-	-	-	-	-	-	-
0.0117	0.109	0.116	0.120	0.125	-	-	-	-	-	-	-	-	-	-	-	-
0.0125	0.116	0.122	-	-	-	-	-	-	-	-	-	-	-	-	-	-

Table 6. Comparison of depth and specific energy in section B in single and double sill state for the tangential sill mode

Tangential sill mode

Q(m³/s)	B=2.5 cm				B=5 cm				B=7.5 cm				B=10 cm			
	Single sill		Double sill		Single sill		Double sill		Single sill		Double sill		Single sill		Double sill	
	y_B	E_B	y_B	E_B	y_B	E_B	y_B	E_B	y_B	E_B	y_B	E_B	y_B	E_B	y_B	E_B
0.0075	-	-	-	-	-	-	-	-	-	-	-	-	0.065	0.073	0.064	0.072
0.0083	0.062	0.072	0.063	0.073	0.065	0.074	0.065	0.074	0.069	0.078	0.067	0.076	0.073	0.080	0.070	0.078
0.0092	0.071	0.081	0.070	0.080	0.073	0.082	0.073	0.082	0.076	0.084	0.075	0.083	0.080	0.087	0.078	0.086
0.0096	-	-	-	-	-	-	-	-	-	-	-	-	-	-	-	-
0.0100	0.078	0.088	0.077	0.087	0.081	0.090	0.078	0.087	0.086	0.093	0.081	0.090	0.088	0.095	0.087	0.095
0.0104	-	-	-	-	0.085	0.090	-	-	-	-	-	-	-	-	-	-
0.0108	0.085	0.094	0.085	0.094	0.088	0.097	0.088	0.096	0.092	0.100	0.091	0.099	0.096	0.104	0.096	0.103
0.0113	0.088	0.097	-	-	0.093	0.101	-	-	0.095	0.103	-	-	-	-	-	-
0.0117	0.093	0.102	0.095	0.103	0.096	0.104	0.097	0.105	0.098	0.106	0.099	0.107	0.103	0.111	0.104	0.111
0.0125	0.099	0.108	0.101	0.109	0.103	0.111	0.103	0.111	0.107	0.115	0.107	0.115	0.112	0.119	0.112	0.119
0.0133	0.108	0.117	0.108	0.116	0.112	0.120	0.111	0.119	0.114	0.122	0.114	0.122	0.119	0.126	0.120	0.127
0.0142	0.116	0.125	0.115	0.123	0.118	0.126	0.119	0.126	0.122	0.130	0.123	0.130	0.126	0.133	0.128	0.135

Q(m³/s)	B=15 cm				B=20 cm				B=25 cm				B=30 cm			
	Single sill		Double sill		Single sill		Double sill		Single sill		Double sill		Single sill		Double sill	
	y_B	E_B	y_B	E_B	y_B	E_B	y_B	E_B	y_B	E_B	y_B	E_B	y_B	E_B	y_B	E_B
0.0042	-	-	-	-	-	-	-	-	-	-	-	-	0.053	0.057	0.057	0.060
0.0046	-	-	-	-	-	-	-	-	-	-	-	-	0.063	0.066	0.063	0.066
0.0050	-	-	-	-	-	-	-	-	0.055	0.059	0.055	0.060	0.067	0.070	0.068	0.071
0.0058	-	-	-	-	-	-	-	-	0.064	0.068	0.066	0.071	0.081	0.084	0.081	0.083
0.0063	-	-	-	-	-	-	-	-	-	-	-	-	0.086	0.089	0.087	0.090
0.0067	-	-	-	-	-	-	-	-	0.078	0.089	0.077	0.081	0.092	0.095	0.092	0.095
0.0075	0.071	0.077	0.070	0.076	0.078	0.083	0.077	0.082	0.085	0.087	0.085	0.090	-	-	-	-
0.0079	-	-	-	-	-	-	-	-	-	-	-	-	-	-	-	-
0.0083	0.079	0.085	0.078	0.085	0.084	0.090	0.085	0.090	0.092	0.097	0.093	0.098	-	-	-	-
0.0092	0.086	0.093	0.087	0.093	0.096	0.101	0.094	0.099	0.100	0.105	0.101	0.106	-	-	-	-
0.0096	-	-	-	-	-	-	-	-	0.105	0.110	0.106	0.110	-	-	-	-
0.0100	0.094	0.100	0.095	0.101	0.104	0.109	0.104	0.109	-	-	-	-	-	-	-	-
0.0108	0.102	0.109	0.103	0.110	0.113	0.119	0.114	0.119	-	-	-	-	-	-	-	-
0.0113	0.107	0.113	-	-	-	-	-	-	-	-	-	-	-	-	-	-
0.0117	0.111	0.117	0.112	0.118	0.121	0.126	0.119	0.124	-	-	-	-	-	-	-	-

3.10. Investigating the hydraulic parameters of hydraulic jump with triple sill state

The specific energy values in sections A and B for the case of triple sills under the gate position and upstream tangent position are presented in Tables (7 and 8). By comparing the under tangential sill positions in the mentioned tables, the specific energy in both sections is higher in the under gate position than in the tangent position. The greatest amount of changes is in the specific energy of section A in the under gate position, which reduces the depth of the flow in that section. Therefore, this process leads to a change in the fluid depth in section B, so that the depth under the gate position is greater than the tangent one, which indicates an increase in specific energy in section B.

Table 7. The specific energy of the hydraulic jump of sections A and B with the triple sill state under the gate position

Under gate sill mode

Q(m³/s)	B=2.5 cm		B=5 cm		B=7.5 cm		B=10 cm		B=15 cm		B=20 cm		B=25 cm		B=30 cm	
	E_A	E_B	E_A	E_B	E_A	E_B	E_A	E_B	E_A	E_B	E_A	E_B	E_A	E_B	E_A	E_B
0.0038	-	-	-	-	-	-	-	-	-	-	-	-	-	-	0.137	0.057
0.0042	-	-	-	-	-	-	-	-	-	-	-	-	0.112	0.047	0.178	0.063
0.0050	-	-	-	-	-	-	-	-	-	-	-	-	0.156	0.065	0.266	0.076
0.0058	-	-	-	-	-	-	-	-	-	-	-	-	0.222	0.079	-	-
0.0067	-	-	-	-	-	-	-	-	0.116	0.073	0.176	0.076	0.321	0.092	-	-
0.0075	-	-	-	-	-	-	0.095	0.074	0.132	0.077	0.205	0.085	0.400	0.103	-	-
0.0083	-	-	0.097	0.075	0.106	0.077	0.119	0.082	0.149	0.087	0.239	0.094	-	-	-	-
0.0092	0.104	0.079	0.113	0.082	0.126	0.084	0.142	0.087	0.153	0.094	0.283	0.104	-	-	-	-
0.0100	0.119	0.086	0.131	0.088	0.147	0.092	0.165	0.097	0.215	0.105	0.337	0.114	-	-	-	-
0.0108	0.138	0.094	0.154	0.096	0.200	0.101	0.190	0.105	0.302	0.117	0.405	0.126	-	-	-	-
0.0117	0.156	0.102	0.178	0.106	0.216	0.109	0.217	0.114	0.348	0.126	-	-	-	-	-	-
0.0125	0.176	0.108	0.194	0.113	0.233	0.117	0.263	0.123	-	-	-	-	-	-	-	-
0.0133	0.203	0.117	0.227	0.122	0.251	0.126	0.354	0.131	-	-	-	-	-	-	-	-
0.0142	0.224	0.124	0.266	0.130	0.318	0.135	-	-	-	-	-	-	-	-	-	-

Table 8. The specific energy of the hydraulic jump of sections A and B with the triple sill tangent position

Tangential sill mode

Q(m³/s)	B=2.5 cm		B=5 cm		B=7.5 cm		B=10 cm		B=15 cm		B=20 cm		B=25 cm		B=30 cm	
	E_A	E_B	E_A	E_B	E_A	E_B	E_A	E_B	E_A	E_B	E_A	E_B	E_A	E_B	E_A	E_B
0.0038	-	-	-	-	-	-	-	-	-	-	-	-	-	-	0.136	0.055
0.0042	-	-	-	-	-	-	-	-	-	-	-	-	-	-	0.159	0.058
0.0050	-	-	-	-	-	-	-	-	-	-	-	-	0.093	0.060	0.225	0.071
0.0058	-	-	-	-	-	-	-	-	-	-	-	-	0.134	0.071	0.304	0.082
0.0067	-	-	-	-	-	-	-	-	0.091	0.069	0.102	0.074	0.179	0.079	-	-
0.0075	-	-	-	-	-	-	0.092	0.071	0.116	0.077	0.124	0.083	0.234	0.091	-	-
0.0083	-	-	-	-	0.095	0.077	0.106	0.079	0.133	0.085	0.155	0.090	0.317	0.100	-	-
0.0092	0.104	0.079	0.104	0.080	0.112	0.083	0.125	0.085	0.167	0.092	0.200	0.099	0.394	0.109	-	-
0.0100	0.119	0.086	0.120	0.087	0.138	0.090	0.149	0.092	0.194	0.100	0.219	0.107	-	-	-	-
0.0108	0.138	0.094	0.139	0.095	0.162	0.098	0.175	0.104	0.211	0.109	0.257	0.117	-	-	-	-
0.0117	0.156	0.102	0.176	0.103	0.183	0.107	0.203	0.111	0.278	0.119	0.322	0.126	-	-	-	-
0.0125	0.176	0.108	0.199	0.109	0.215	0.113	0.251	0.119	0.305	0.124	-	-	-	-	-	-
0.0133	0.203	0.117	0.223	0.118	0.241	0.122	0.260	0.128	-	-	-	-	-	-	-	-
0.0142	0.224	0.124	0.249	0.125	-	-	0.292	0.132	-	-	-	-	-	-	-	-

3.11. Presenting regression relationships

In this research, to predict the relative energy dissipation, equations were presented within the scope of this research. The way of choosing the equations was by determining the corresponding values of the dimensionless parameters and combining the mentioned data, the equations were calculated according to the following process:

First, the nonlinear form for the proposed equations of relative energy dissipation was determined as a function of dimensionless parameters. The proposed equations were presented using Solver in Excel software to achieve their appropriate form and with the least amount of error in the form of Equations (8 and 9) for the no-sill state:

$$\frac{\Delta E_{AB}}{E_A} = -1{,}617 Fr_A^{-0{,}574} + 1{,}212 \left(\frac{G}{y_A}\right)^{0{,}00031} + 0{,}487 \left(\frac{y_B}{y_A}\right)^{-12{,}355} - 19{,}697 \left(\frac{L_j}{y_A}\right)^{-81{,}497} \tag{8}$$

$$\frac{\Delta E_{AB}}{E_B} = 0{,}817 Fr_A^{1{,}003} - 0{,}0003 \left(\frac{G}{y_A}\right)^{0{,}582} - 0{,}371 \left(\frac{y_B}{y_A}\right)^{0{,}957} - 0{,}485 \left(\frac{L_j}{y_A}\right)^{0{,}185} \tag{9}$$

In Figures (11-a and c), a comparison of the calculated and experimental values of relative energy dissipation is drawn. The trend of changes in the relative energy dissipation from the experimental results is the same as the values obtained from the equations. The results of the R^2, RMSE, and KGE indicators are 0.997, 0.0108, and 0.998, respectively, comparing the experimental results with Equation (8). In addition, the mentioned indicators for the ratio of energy dissipation to downstream specific energy are 1, 0.0073, and 1, respectively (Figure 11-c). According to Figures (11-b and d), independent parameter y_B/y_A and dependent parameters $\Delta E_{AB}/E_A$ and $\Delta E_{AB}/E_B$ have been investigated to check the accuracy of Equations (8) and (9). In Figures (11-b and d), the percentage relative error against the effective dimensionless parameter y_B/y_A is shown. In Figure (11-b), a wide range of data is placed in the relative error band of $\pm 5\%$. So more than 88% of the data have a relative error of less than $\pm 5\%$. In Figure (11-d), more than 88% of the data are within the relative error range of $\pm 1\%$. This shows that the proposed equations have a very favorable accuracy in predicting the relative energy dissipation.
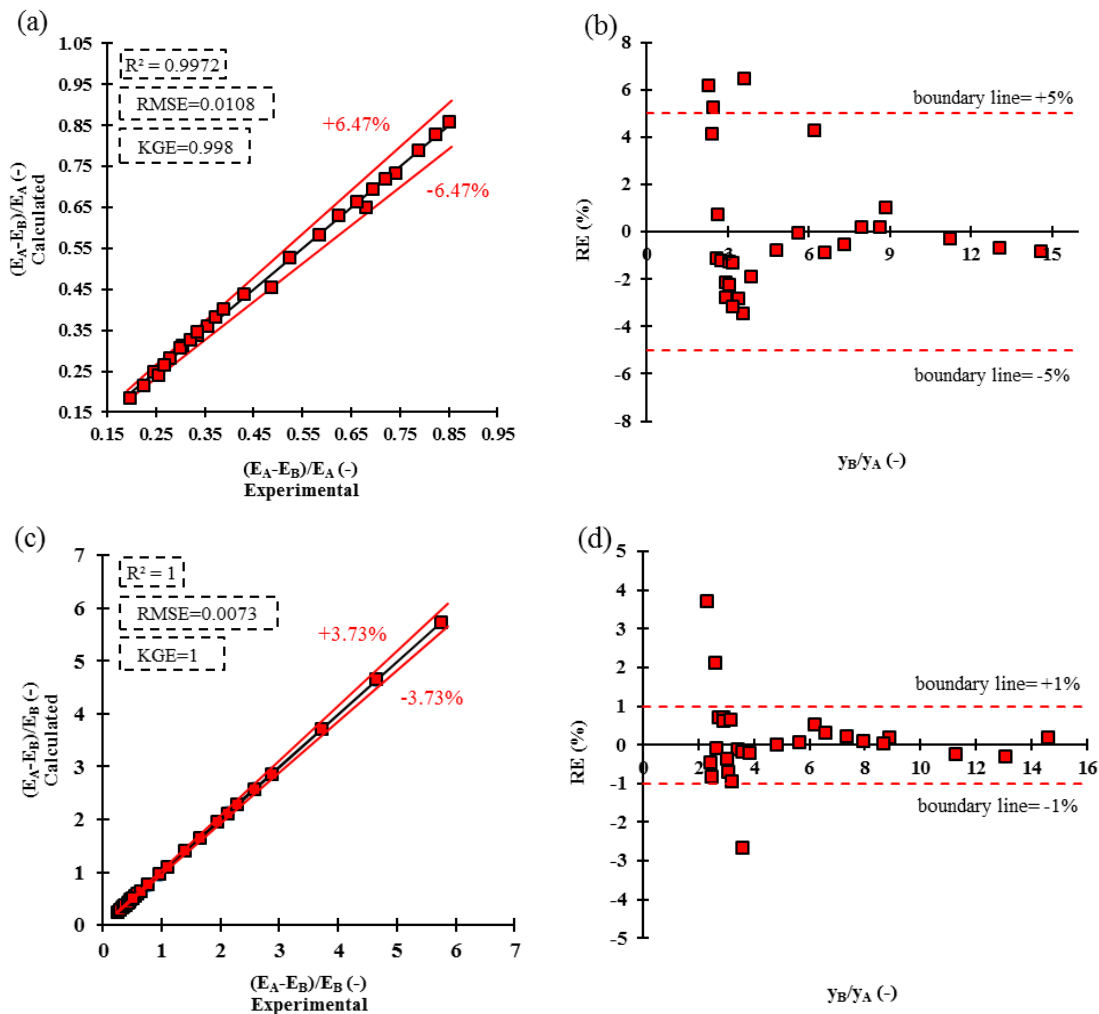

Figure 11. a, c) Comparison of calculated and experimental values of the ratio of energy dissipation to upstream and downstream specific energy b, d) Scatter diagram of relative data error

To predict the ratio of energy dissipation to the upstream and downstream specific energy in the sill state, Equations (10 and 11) are presented, respectively.

$$\frac{\Delta E_{AB}}{E_A} = -3{,}067 Fr_A^{-0{,}778} + 1{,}692 \left(\frac{y_B}{y_A}\right)^{-1{,}073} + 0{,}004 \left(\frac{B}{y_A}\right)^{-9{,}083} + 1{,}161 \left(\frac{B}{y_B}\right)^{0{,}001} \tag{10}$$

$$\frac{\Delta E_{AB}}{E_B} = 0{,}486 Fr_A^{1{,}180} - 0{,}175 \left(\frac{y_B}{y_A}\right)^{1{,}228} + 0{,}012 \left(\frac{B}{y_A}\right)^{-6{,}197} - 0{,}537 \left(\frac{B}{y_B}\right)^{0{,}008} \tag{11}$$

Figure (12) shows the comparison of the experimental results with the calculation results for the ratio of energy dissipation to the upstream and downstream specific energy. The results of the statistical indicators of the maximum percentage relative error, the mean percentage relative error, and the root mean square error of comparing the results between experimental data with Equation (10) are 8.53%, 0.78%, and 0.004, respectively. In addition, the KGE index for Equation (10) is in the very good range. The results of statistical indicators for Equation (11) are 12.15%, 0.87%, and 0.009, respectively. The KGE index for Equation (11) is very good.
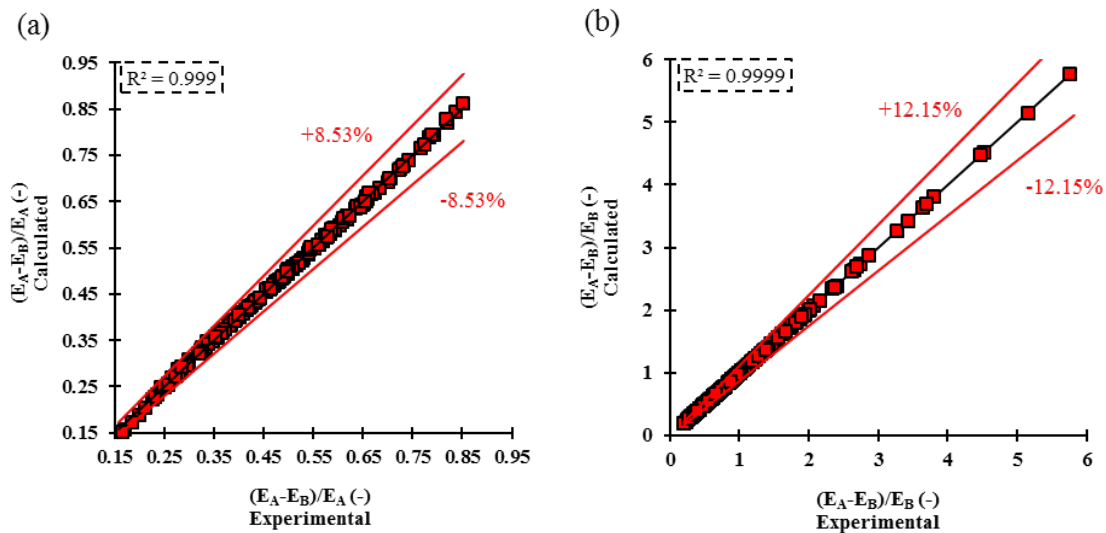
Figure 12. Comparison of experimental and calculated values of energy dissipation relative to a) upstream specific energy b) downstream specific energy

In Table (9), the range of the $\Delta E_{AB}/E_A$ values and various Fr_A from the present research with single sill mode with different sill positions are compared with the results of the previous studies including Jalil et al. [9] and Daneshfaraz et al. [21]. It should be noted that in studies Jalil et al. [9] and Daneshfaraz et al. [21], the sill is only located below the gate. While in this research, different positions of sill have been investigated. The scope of investigation of Froude number and relative energy dissipation in the current research has been carried out in a wider range than other research.

Table 9. Results of the $\Delta E_{AB}/E_A$ of the present research with previous studies

Case	Type of Sill (Z=0.03 m)	Range of Fr_A (-)	Range of $\Delta E_{AB}/E_A$ (-)
Jalil et al. [9]	Prismatic Sill	$2.41 \le Fr_A \le 5.76$	$0.14 \le \Delta E_{AB}/E_A \le 0.59$
Daneshfaraz et al. [21]	Triangular	$2.47 \le Fr_A \le 7.49$	$0.20 \le \Delta E_{AB}/E_A \le 0.67$
Present Study (under gate position)	Rectangular	$2.40 \le Fr_A \le 12.42$	$0.20 \le \Delta E_{AB}/E_A \le 0.84$
Present Study (upward tangent position)	Rectangular	$2.23 \le Fr_A \le 12.11$	$0.17 \le \Delta E_{AB}/E_A \le 0.82$
Present Study (downward tangent position)	Rectangular	$2.14 \le Fr_A \le 9.51$	$0.25 \le \Delta E_{AB}/E_A \le 0.77$

4. Conclusion

In the present study, the hydraulic characteristics of the hydraulic jump in different openings of the sluice gate in the no-sill and with sill states were investigated experimentally in various widths and positions relative to the gate. In a specific opening, the application of the sill in the below and tangential positions leads to more energy dissipation. As the ratio of initial depth to sequent depth increases, the value of $\Delta E_{AB}/y_A$ decreases. This happens due to the convergence of the initial and sequent depths so increasing the initial depth leads to the formation of a weak jump and low energy dissipation. By comparing the amount of relative energy dissipation in all three cases of a single sill at positions under the gate and tangent to the gate upstream and downstream, the case under the gate has more energy dissipation than other cases of sill application. In all positions, the ratio of energy dissipation to upstream and downstream specific energy decreases with increasing gate opening. In the same opening in the case of no-sill and with a single sill, the use of a suppressed sill in the below and tangent position upstream and downstream leads to a decrease in the sequent depth compared to the no-sill state. The application of the sill compared to the no-sill state causes an increase in the initial depth; accordingly, the initial specific energy decreases; therefore, the application of the sill leads to the reduction of the specific energy in the conjugate depths.

References

1. Kubrak E, Kubrak J, Kiczko A, Kubrak M, (2020). Flow measurements using a sluice gate; analysis of applicability. Water, 12(3): 819.
2. Pástor M, Bocko J, Lengvarský P, Sivák P, Šarga P, (2020). Experimental and Numerical Analysis of 60-Year-Old Sluice Gate Affected by Long-Term Operation. Materials, 13(22): 5201. https://doi.org/10.3390/ma13225201
3. Daneshfaraz R. Abbaszadeh H, Gorbanvatan P, Abdi M, (2021). Application of Sluice Gate in Different Positions and Its Effect on Hydraulic Parameters in Free-Flow Conditions. Journal of Hydraulic Structures, 7: 72–87. https://doi.org/10.22055/jhs.2022.39208.1196.
4. Yoosefdoost A, Lubitz W.D, (2022). Sluice Gate Design and Calibration: Simplified Models to Distinguish Flow Conditions and Estimate Discharge Coefficient and Flow Rate. Water, 14(8): 1215. https://doi.org/10.3390/w14081215
5. Alhamid AA, (1999). Coefficient of Discharge for Free Flow Sluice Gates. Journal of King Saud University - Engineering Sciences, 11(1): 33-47.
6. Salmasi F, Abraham J, (2020). Prediction of Discharge Coefficients for Sluice Gates Equipped with Different Geometric Sills under the Gate Using Multiple non-linear Regression (MNLR). Journal of Hydrology. DOI: 10.1016/j.jhydrol.2020.125728.

7. Ghorbani M.A, Salmasi F, Saggi M.K, Bhatia A.S, Kahya E, Norouzi R, (2020). Deep Learning under H_2O Framework: A Novel Approach for Quantitative Analysis of Discharge Coefficient in Sluice Gates. Journal of Hydroinformatics, 22(6): 1603-1619.

8. Daneshfaraz R, Norouzi R, Abbaszadeh H, Kuriqi A, Di Francesco S, (2022). Influence of Sill on the Hydraulic Regime in Sluice Gates: An Experimental and Numerical Analysis. Fluids, 7(7): 244. https://doi.org/10.3390/fluids7070244

9. Jalil S, Sarhan A.S, Yaseen M.S, (2015). Hydraulic Jump Properties Downstream a Sluice Gate with Prismatic Sill. Research Journal of Applied Sciences, Engineering and Technology, 11(4): 447-453.

10. Abdelmonem Y.K, Shabayek S, Khairy A.O, (2018). Energy Dissipation Downstream Sluice Gate Using a Pendulum Sill. Alexandria Engineering Journal, 57(4): 3977-3983.

11. Habibzadeh A, Rajaratnam N, Loewen M, (2019). Characteristics of the Flow Field Downstream of Free and Submerged Hydraulic Jumps. Proceedings of the Institution of Civil Engineers-Water Management, 172(4): 180–194.

12. Ghaderi A, Dasineh M, Aristodemo F, Ghahramanzadeh A, (2020). Characteristics of free and submerged hydraulic jumps over different macroroughnesses. Journal of Hydroinformatics, 22(6): 1554–1572.

13. Harada S, Li S.S, (2018). Modelling hydraulic jump using the bubbly two-phase flow method. Environmental Fluid Mechanics, 18: 335–356. https://doi.org/10.1007/s10652-017-9549-5

14. Chern M.J, Syamsuri S, (2013). Effect of corrugated bed on hydraulic jump characteristic using SPH method. Journal of Hydraulic Engineering, 139(2): 221-232.

15. Raju R, (1984). Scale Effects in Analysis of Discharge Characteristics of Weir and Sluice Gates; Kobus: Esslingen am Neckar, Germany.

16. Lauria A, Calomino F, Alfonsi G, D'Ippolito A, (2020). Discharge Coefficients for Sluice Gates Set in Weirs at Different Upstream Wall Inclinations. Water, 12(1): 245.

17. Daneshfaraz R, Norouzi R, Abbaszadeh H, Azamathulla H.M, (2022). Theoretical and experimental analysis of applicability of sill with different widths on the gate discharge coefficients. Water Supply, 22(10): 7767–7781. doi: https://doi.org/10.2166/ws.2022.354.

18. Norouzi R, Sihag P, Daneshfaraz R, Abraham J, Hasannia V, (2021). Predicting relative energy dissipation for vertical drops equipped with a horizontal screen using soft computing techniques. Water Supply, 21(8): 4493-4513.

19. Nasrabadi M, Mehri Y, Ghassemi A, Omid M.H, (2021). Predicting Submerged Hydraulic Jump Characteristics Using Machine Learning Methods. Water Supply, 21(8): 4180–4194.

20. Gupta H.V, Kling H, Yilmaz K.K, Martinez G.F, (2009). Decomposition of the mean squared error and NSE performance criteria: Implications for improving hydrological modelling. J. Hydrol, 377(1-2): 80–91.

21. Daneshfaraz R, Norouzi R, Ebadzadeh P, Di Francesco S, Abraham J.P, (2023). Experimental Study of Geometric Shape and Size of Sill Effects on the Hydraulic Performance of Sluice Gates. Water, 15(2): 314. https://doi.org/10.3390/w15020314.